The Eurasia Proceedings of Science, Technology, Engineering and Mathematics (EPSTEM)
ISSN: 2602-3199

The Eurasia Proceedings of Science, Technology, Engineering and Mathematics (EPSTEM), 2026

Volume 40, Pages 129-139

ICBAST 2026: International Conference on Basic Sciences and Technology

Comparative Analysis of Earthquake-Induced Hydrodynamic Pressures in Dam–Reservoir Systems Using CFD and Analytical Methods

Ali Yildiz
Konya Technical University

Gulnaz Donmez
Konya Technical University

Mustafa Kocer
Konya Technical University

Abstract: Hydrodynamic pressures induced by earthquake excitation constitute a critical load component in the seismic safety assessment of dam–reservoir systems. In this study, earthquake-induced dynamic pressures acting on a rigid dam face were investigated numerically and compared with classical analytical approaches. A three-dimensional reservoir model with dimensions of 3 m × 3 m × 4 m was established in ANSYS Fluent, and an initial water depth of 2.5 m was defined. The fluid domain was discretized using 5 cm cubic cells, resulting in 288000 elements. A two-phase flow model was employed, and the free-surface motion was tracked using the Volume of Fluid (VOF) method under transient conditions. As seismic input, the East–West component of the February 6 Kahramanmaraş earthquake record obtained from the Göksun station (No: 4612) was used. The strong-motion interval of the record was applied in the numerical analyses. The pressure distributions obtained from the computational fluid dynamics (CFD) model were compared with the results of the Westergaard, Von Kármán, and Zangar methods. The numerical results indicated that the location and magnitude of peak hydrodynamic pressures varied with time, whereas the classical analytical methods generally predicted the maximum pressure at the dam base. The findings show that classical methods may provide practical and conservative estimates for overall loading, while CFD analysis offers a more detailed representation of time-dependent local pressure concentrations on the dam surface.

Keywords: Hydrodynamic pressure, Dam-reservoir interaction, CFD, Seismic loading, ANSYS Fluent

Introduction

Dams are among the most critical hydraulic structures, serving essential functions in water storage, irrigation, hydroelectric power generation, flood control, and water resources management. Because of their large dimensions and the potentially severe consequences of failure, their structural safety under extreme loading conditions is of great importance. Seismic effects are particularly critical in this regard, as earthquake excitation can significantly alter the stress state of the dam body and the hydrodynamic behavior of the reservoir. During an earthquake, the relative motion between the dam and the impounded water generates additional hydrodynamic pressures on the upstream face, superimposed on the existing hydrostatic pressure. Therefore, a reliable estimation of these earthquake-induced hydrodynamic loads is essential for the seismic assessment and safe design of dam–reservoir systems (Jawad et al., 2021; Goldaran, 2022; Ye et al., 2023).

The seismic behavior of dam–reservoir systems has long been investigated using analytical methods developed under simplified physical assumptions. The pioneering work of Westergaard (1933) introduced the "added-mass" concept and provided the first rational analytical solution for hydrodynamic pressure acting on a rigid dam with a

- Selection and peer-review under responsibility of the Organizing Committee of the Conference

vertical upstream face under horizontal ground motion. Subsequently, Von Kármán (1933) examined the same problem through a momentum-based formulation, proposing a simplified alternative suitable for engineering calculations. Later, Zangar (1953) extended this framework by introducing empirical pressure coefficients for both vertical and inclined upstream faces, thereby improving the applicability of analytical calculations to practical dam geometries. More advanced studies, such as those by Housner (1957) and Chopra (1967), further refined the physical representation of the problem by considering impulsive and convective components, sloshing effects, fluid compressibility, and dam flexibility. These studies collectively form the theoretical foundation of modern dam–reservoir interaction analysis (Westergaard, 1933; Von Kármán, 1933; Zangar, 1953; Housner, 1957; Chopra, 1967). Despite their practical value, classical analytical methods rely on several simplifying assumptions, such as rigid dam behavior, incompressible and inviscid fluid motion, and idealized pressure distributions that are generally expressed only as a function of water depth. These assumptions make the methods attractive for rapid preliminary evaluation; however, they may not fully capture the transient and spatially varying nature of hydrodynamic pressures under real earthquake records. In particular, local pressure concentrations, temporal phase changes, and free-surface effects may not be adequately represented by simplified closed-form solutions. For this reason, numerical approaches have become increasingly important in recent years, especially in studies where fluid–structure interaction and time-dependent pressure evolution must be evaluated in greater detail (Goldaran, 2022; Ye et al., 2023).

In this context, Computational Fluid Dynamics (CFD) offers a robust framework for simulating transient fluid motion and evaluating hydrodynamic pressure distributions on dam surfaces under seismic excitation. Addressing this need, the present study investigates earthquake-induced hydrodynamic pressures acting on a rigid dam face using a three-dimensional CFD model developed in ANSYS Fluent. The numerical results are compared with the classical analytical approaches of Westergaard, Von Kármán, and Zangar in terms of pressure magnitude and distribution. Thus, the study aims to assess the applicability of widely used classical methods for practical engineering calculations and to demonstrate the contribution of CFD-based modeling to a more refined understanding of dam–reservoir interaction under earthquake loading.

Method

Analytical Calculation Approaches

The analytical component of this study is strategically established to serve as a rigorous benchmark for evaluating and validating the numerical results derived from the Computational Fluid Dynamics (CFD) model. In the field of dam engineering, while numerical methods offer high spatial resolution, their accuracy is inherently dependent on factors such as mesh convergence, turbulence modeling, and temporal discretization; therefore, comparing these results with established theoretical solutions is a critical step in ensuring the reliability of the CFD simulation. To this end, three classical approaches—the Westergaard (1933), Von Kármán (1933) and Zangar (1953) methods—were selected for this comparative framework due to their widespread adoption in international design codes and their reliance on deterministic, closed-form, or semi-empirical formulations. These methods remain the cornerstone of seismic dam analysis, providing a clear mathematical baseline that is free from the numerical oscillations often encountered in transient simulations. The primary objective of employing these analytical formulations is to systematically determine the hydrodynamic pressure distribution across the vertical profile of the dam, the resultant hydrodynamic force, and the precise location of the pressure center. By calculating these parameters under controlled conditions, a direct point-by-point comparison can be performed against the transient pressure data extracted from ANSYS Fluent, thereby not only validating the CFD model's predictive capability but also highlighting the specific conditions under which classical assumptions may deviate from the complex fluid behavior captured by the Navier-Stokes equations.

Common Assumptions

The analytical framework adopted in this study is predicated on several idealized physical assumptions that define the interaction between the reservoir fluid and the dam structure. In the selected approaches of Westergaard (1933), Von Kármán (1933), and Zangar (1953), the reservoir water is treated as an incompressible, inviscid, and irrotational fluid, thereby neglecting the effects of internal friction and potential energy dissipation within the fluid medium. The seismic excitation is characterized as a purely horizontal ground acceleration acting on the dam–reservoir system, with the dam body itself idealized as a perfectly rigid structure. Consequently, the analysis focuses on the hydrodynamic pressure generated by the rigid-body motion of the dam face against the impounded water, rather than the complex deformations involving dam flexibility. While the formulations of Westergaard

(1933) and Von Kármán (1933) are specifically constrained to a vertical upstream face, the Zangar (1953) method extends this applicability by incorporating empirical pressure coefficients that account for various upstream face inclinations. These fundamental simplifications allow for the derivation of depth-dependent pressure distributions, providing a consistent and common analytical basis for the comparative evaluation of the transient numerical results obtained in this study.

Notation

In the analytical formulations, ρ denotes the water density, a_g is the horizontal ground acceleration, y is the depth variable used in the analytical formulations along the upstream dam face, and h is the total water depth. In addition, $m_a(y)$ represents the equivalent added mass per unit width at depth y, $p(y)$ is the hydrodynamic pressure, S_0 is the resultant hydrodynamic force, and y_c is the location of the pressure center. In the Zangar formulation, C_h denotes the hydrodynamic pressure coefficient associated with the upstream dam-face geometry.

Westergaard Method (1933)

The Westergaard method is one of the earliest analytical approaches developed for evaluating earthquake-induced hydrodynamic pressures on rigid dams. The method is based on the added-mass concept and assumes that a portion of the reservoir water moves together with the rigid dam face during horizontal earthquake excitation. Under the assumptions of incompressible and inviscid fluid motion, rigid dam behavior, and a vertical upstream face, the hydrodynamic pressure distribution can be expressed as follows.

According to Westergaard, the depth-dependent added mass distribution is given by Equation (1).

$$m_a(y) = \frac{7}{8}\rho\sqrt{yh} \tag{1}$$

The hydrodynamic pressure is obtained by multiplying the added mass by the horizontal ground acceleration, as given in Equation (2).

$$p(y) = m_a(y)a_g \tag{2}$$

Thus, the hydrodynamic pressure distribution can be written as Equation (3).

$$p(y) = \frac{7}{8}\rho a_g\sqrt{yh} \tag{3}$$

In this approach, the pressure center is generally taken at approximately two-fifths of the water depth from the dam base.

Von Kármán Method (1933)

The Von Kármán method evaluates earthquake-induced hydrodynamic pressure by using a momentum-based analytical formulation. Similar to the Westergaard approach, the method assumes that the dam body is rigid, the reservoir fluid is incompressible and inviscid, and the excitation acts horizontally. However, the equivalent added-mass distribution is represented by a different expression, which leads to a modified pressure profile along the dam face.

According to the Von Kármán formulation, the depth-dependent added mass distribution is given by Equation (4).

$$m_a(y) = \rho\left(\frac{4}{3}\sqrt{yh} - \frac{y^2}{h}\right) \tag{4}$$

The hydrodynamic pressure is obtained from Equation (5).

$$p(y) = m_a(y)a_g \tag{5}$$

Thus, the pressure distribution becomes Equation (6).

$$p(y) = \rho a_g \left(\frac{4}{3}\sqrt{yh} - \frac{y^2}{h}\right) \tag{6}$$

The resultant hydrodynamic force acting on the dam face is expressed by Equation (7).

$$S_0 = \frac{5}{8}\rho a_g h^2 \tag{7}$$

The pressure center is taken as Equation (8).

$$y_c = \frac{2}{5}h \tag{8}$$

These expressions show that the Von Kármán approach also predicts a nonlinear hydrodynamic pressure distribution and provides a practical analytical basis for comparison with numerical results.

Zangar Method (1953)

The Zangar method is a practical analytical approach developed for estimating earthquake-induced hydrodynamic pressures on both vertical and inclined dam faces. Unlike the Westergaard and Von Kármán methods, the Zangar formulation introduces an empirical hydrodynamic coefficient to account for the effect of the upstream face geometry. Owing to its simple coefficient-based structure, the method is widely used in engineering practice for approximate evaluation of hydrodynamic pressure, resultant force, and pressure center.

According to the Zangar formulation, the hydrodynamic pressure distribution along the dam face is given by Equation (9).

$$p(y) = C_h \rho g h \left(1 - \frac{y}{h}\right)^{1.5} \tag{9}$$

For a vertical upstream face, the hydrodynamic coefficient is expressed by Equation (10).

$$C_h = 0.726\frac{a_g}{g} \tag{10}$$

For an inclined upstream face, the modified hydrodynamic coefficient is given by Equation (11).

$$C_{h,\alpha} = C_h(1 - 0.01\alpha) \tag{11}$$

The resultant hydrodynamic force acting on the dam face can be approximated by Equation (12).

$$S_0 \approx 0.54\rho a_g h^2 \tag{12}$$

The pressure center is taken as Equation (13).

$$y_c \approx 0.4h \tag{13}$$

These equations indicate that the Zangar method provides a simplified yet practical means of representing earthquake-induced hydrodynamic pressure, particularly when the influence of face inclination needs to be included in the analysis.

Numerical Model

Geometry and Mesh

To evaluate the transient hydrodynamic loads exerted on the dam face during seismic excitation, a three-dimensional numerical simulation was performed using the pressure-based solver in ANSYS Fluent. The computational domain was designed to represent a discretized reservoir volume with dimensions of 3 m×3 m×4 m (L×W×H). To define the fluid-structure interface and the reservoir boundaries, all peripheral surfaces of the domain were characterized as rigid wall boundary conditions. The spatial discretization of the fluid domain was achieved using a structured meshing approach consisting of high-quality hexahedral (cubic) meshs. Each mesh was defined with a uniform edge length of 50 mm (5 cm), ensuring a consistent mesh topology throughout the reservoir. Consequently, the final numerical model comprised a total of 288,000. This specific mesh density was selected after a preliminary sensitivity analysis to provide sufficient spatial resolution for capturing localized pressure gradients while maintaining computational efficiency and manageable processing times. The detailed geometry of the reservoir domain and the corresponding structured mesh configuration utilized in the transient analyses are illustrated in Figure 1.

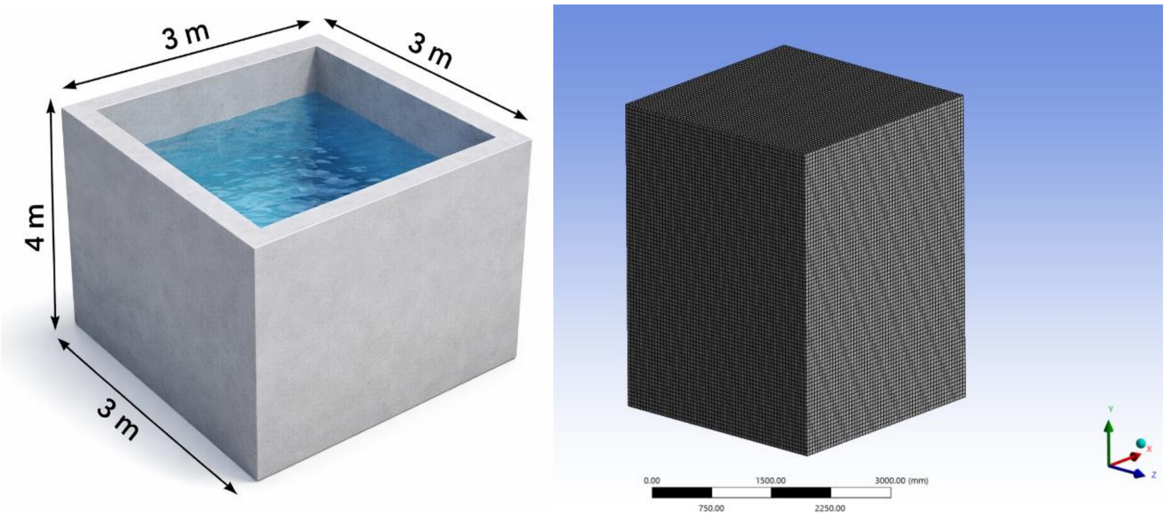

Figure 1. Geometry of the reservoir domain and structured mesh used in the numerical model.

Multiphase Flow Setup

Since the seismic response of the reservoir involves free-surface motion, water and air were defined together by using a two-phase flow model. The transient movement of the free surface was tracked by the Volume of Fluid (VOF) method. At the beginning of the analysis, the initial water level in the reservoir was taken as 2.5 m, and the remaining upper region was assigned as air. In order to ensure numerical stability and to capture the time-dependent fluid motion with sufficient accuracy, small time increments in the range of 0.01–0.005 s were used throughout the transient analyses. The initial water level and the two-phase water–air configuration adopted in the numerical model are shown in Figure 2.

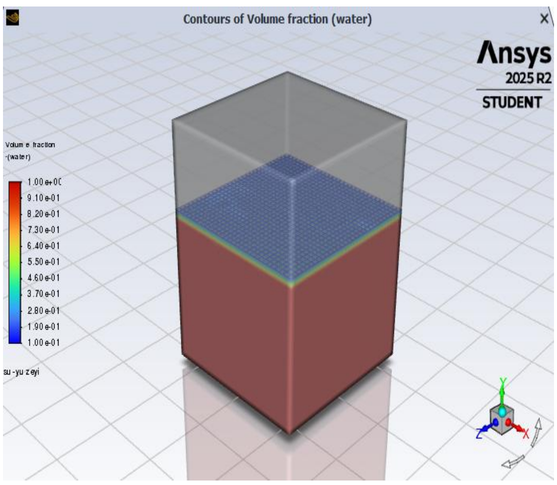

Figure 2. Initial water level and two-phase water–air setup used in the VOF-based numerical model.

Seismic Input

The seismic excitation utilized in the numerical simulations was derived from the East–West (E-W) acceleration-time history recorded at the Kahramanmaraş/Göksun station (Station No: 4612) during the catastrophic earthquake of February 6, 2023. Within the computational framework, gravitational acceleration was consistently applied in the negative Y-direction as g=9.81 m/s2. The real-world earthquake-induced acceleration record was prescribed in the positive X and Z directions to evaluate the multidimensional hydrodynamic response of the reservoir. To optimize computational resources while capturing the most significant seismic effects, the analysis focused on the "strong-motion" interval of the record. Specifically, the 20-second window between t=25 s and t=45 s, representing the peak seismic energy release and the highest acceleration amplitudes, was extracted for the transient simulations. The complete acceleration-time history and the delineated strong-motion interval employed in this study are illustrated in Figure 3.

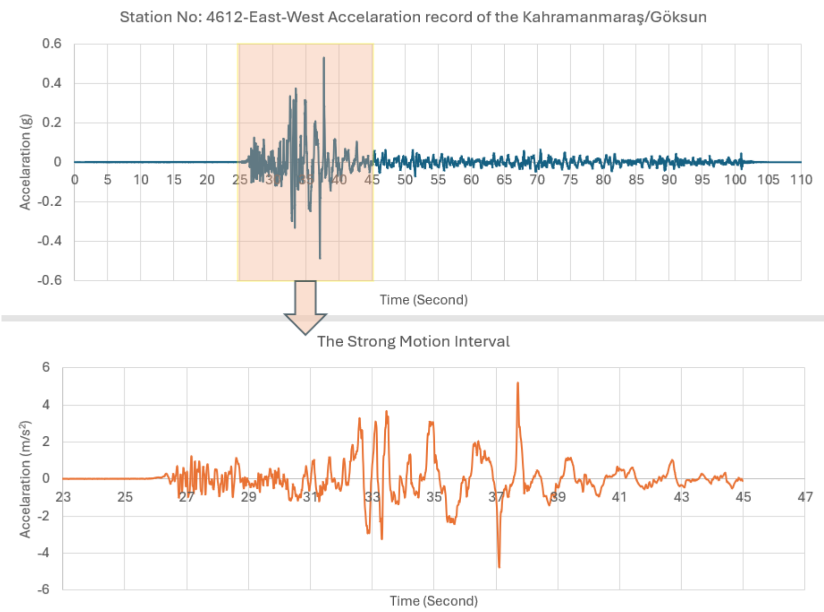

Figure 3. East–West acceleration record of the Kahramanmaraş/Göksun station and the strong-motion interval used in the numerical analyses.

Evaluation Procedure

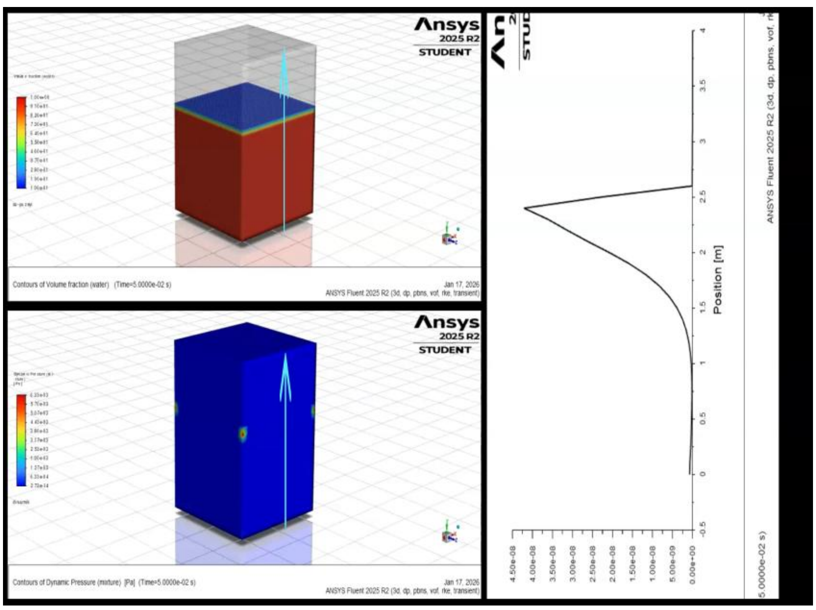

Figure 4. Free-surface response, dynamic pressure contour, and pressure profile extracted along the selected vertical line on the dam wall.

The purpose of the numerical analysis was to determine the time- and depth-dependent hydrodynamic pressure distributions acting on the dam face during earthquake excitation. In addition to the transient free-surface response, the variation of dynamic pressure along the dam wall was monitored throughout the analysis. Pressure values were extracted along a vertical line located on the wall in the Z direction, and the resulting distributions were used for comparison with the analytical methods. According to the obtained results, the highest dynamic pressure values were observed at $t = 15.3$ sand $t = 15.6$ s. Therefore, these critical time steps were selected for comparison with the Westergaard, Von Kármán, and Zangar approaches. The free-surface response, dynamic pressure contour, and the extracted pressure profile along the selected vertical line are illustrated in Figure 4.

Results and Discussion

Pressure Distribution at Critical Times

The transient numerical simulations reveal that the hydrodynamic pressure exerted on the dam face undergoes significant temporal and spatial variations throughout the seismic excitation. Based on the ANSYS Fluent results, the most critical hydrodynamic responses—characterized by peak pressure magnitudes and gradients—were identified at t=30.55 s and t=31.85 s. Consequently, these two specific time instants were selected as the primary focal points for a detailed comparative analysis with the classical analytical approaches. As illustrated in Figure 5, the dynamic pressure distributions derived from the CFD model exhibit a clear time-dependent nature that contrasts with the static profiles of analytical solutions. The numerical curve at t=30.55 s demonstrates a distinct localized peak, whereas the response at t=31.85 s reflects a lower pressure intensity across the majority of the depth range. This discrepancy highlights that the reservoir's hydrodynamic behavior cannot be simplified into a single static pattern; rather, it is intrinsically linked to the instantaneous fluid kinematics, transient oscillations, and free-surface fluctuations captured by the Navier-Stokes equations.

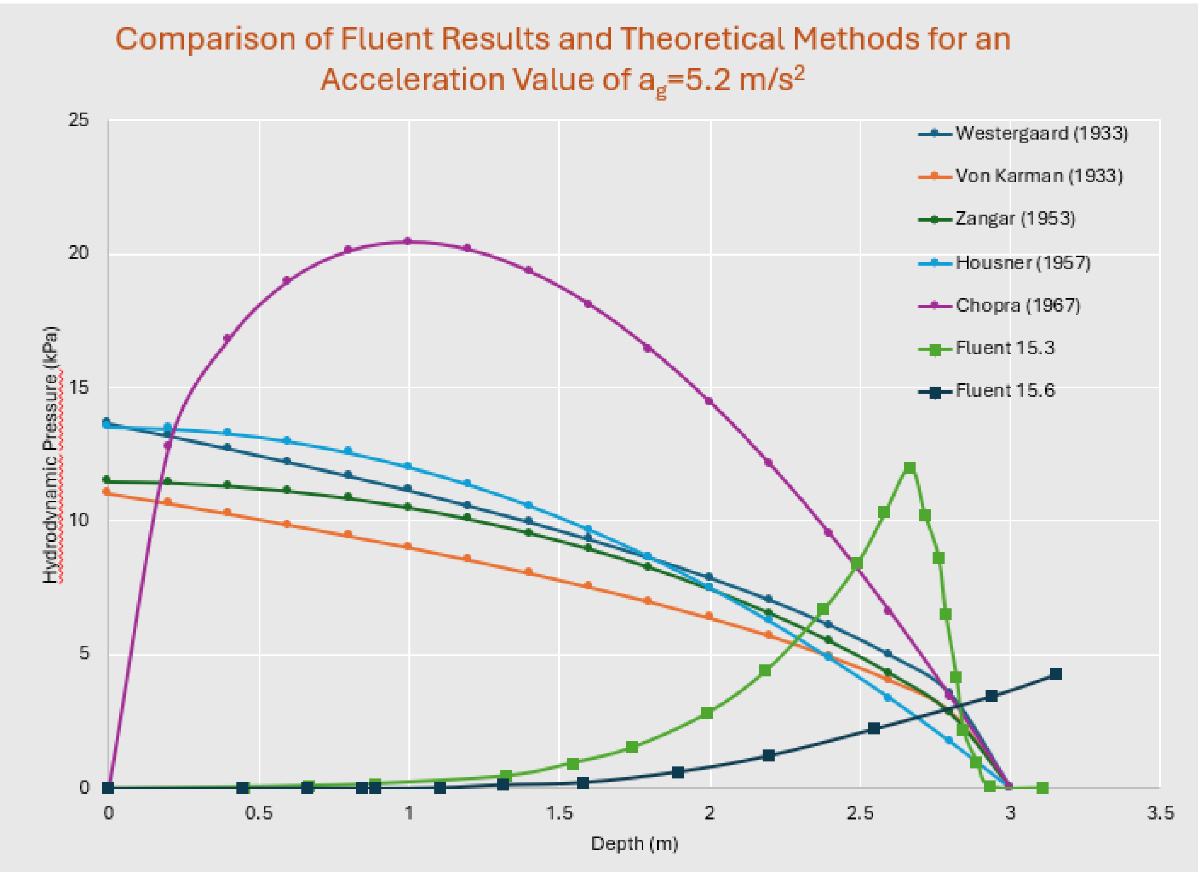

Figure 5. Comparison of dynamic pressure distributions obtained from Theoretical Methods and ANSYS Fluent for $a_g = 5.2$ m/s^2.

Comparison of Analytical and CFD Results

The Westergaard, Von Kármán, and Zangar approaches were compared with the numerical results obtained from ANSYS Fluent in order to evaluate their capability in representing earthquake-induced dynamic pressure on the rigid dam face. In general, all three analytical methods predict smooth depth-dependent pressure distributions derived from simplified assumptions such as rigid dam behavior and idealized fluid response. By contrast, the CFD model captures the transient free-surface motion and the time-dependent development of local pressure concentrations. As summarized in Table 2, the approximate peak dynamic pressure obtained from the Fluent model at $t = 15.3$ sis about 11.9–12.0 kPa, while the secondary critical response at $t = 15.6$ sis about 4.2–4.3 kPa. Among the three analytical methods, Westergaard gives the highest peak value, approximately 13.5–13.6 kPa, whereas Von Kármán and Zangar yield lower peak values of approximately 10.7–10.9 kPa and 11.1–11.3 kPa, respectively. In terms of peak-pressure magnitude, the Von Kármán and Zangar curves are closer to the primary Fluent response than the Westergaard curve. However, the numerical results also show that the location of the peak dynamic pressure changes with time, whereas the analytical methods assume predefined idealized pressure profiles. Therefore, the analytical methods can reproduce the general magnitude level of the dynamic response, but they do not fully capture its transient localization.

Table 2. Approximate peak dynamic pressures read from Figure 5

Method	Approximate peak dynamic pressure (kPa)	Approximate coordinate of peak on plotted axis (m)	General observation
Westergaard (1933)	13.5–13.6	0.0	Smooth, relatively conservative
Von Kármán (1933)	10.7–10.9	0.0	Close to main Fluent peak
Zangar (1953)	11.1–11.3	0.0	Close to main Fluent peak
Fluent 15.3	11.9–12.0	2.65–2.70	Primary critical transient peak
Fluent 15.6	4.2–4.3	3.10–3.15	Secondary critical response

A comparison based on Table 2 indicates that the three analytical methods follow the same general trend as the CFD model in terms of dynamic-pressure level, but the numerical model provides a more realistic description of the spatially localized and time-dependent pressure evolution.

Hydrostatic and Hydrodynamic Force Assessment

To improve the engineering interpretation of the results, the dynamic pressure distributions should be evaluated together with the hydrostatic loading already acting on the dam face. For a vertical wall retaining water, the hydrostatic pressure increases linearly with depth and represents the basic static loading component prior to earthquake excitation. Accordingly, the earthquake-induced hydrodynamic pressure should be interpreted as an additional transient increment superimposed on the pre-existing hydrostatic pressure field.

For the adopted reservoir condition, the initial water depth was taken as $h = 2.5$ m. Based on this water depth, the hydrostatic pressure at the base, the resultant hydrostatic force per unit width, the overturning moment about the base, and the hydrostatic pressure center were calculated analytically. These reference values are given in Table 3.

Table 3. Hydrostatic reference values for $h = 2.5$ m

Quantity	Expression	Value
Base hydrostatic pressure	$p_{h(y)} = \rho g\, y$	24.53 kPa
Resultant hydrostatic force per unit width	$S_h = \frac{1}{2}\rho g h^2$	30.66 kN/m
Overturning moment about base	$M_h = \frac{1}{6}\rho g h^3$	25.55 kN·m/m
Pressure center below free surface	$y_{c,h} = \frac{2h}{3}$	1.67 m
Pressure center above base	$y_{c,h} = \frac{h}{3}$	0.83 m

As seen in Table 3, the hydrostatic component is already significant before the dynamic increment is considered. When the maximum CFD-based dynamic pressure of about 12.0 kPa is compared with the base hydrostatic pressure of 24.53 kPa, it is clear that the hydrodynamic effect acts as a substantial transient addition rather than as the dominant component. In other words, the dynamic peak corresponds to nearly half of the hydrostatic base pressure and should therefore be included in the assessment together with the hydrostatic load. To visually support this interpretation, a simple hydrostatic pressure diagram may be added as Figure 6.

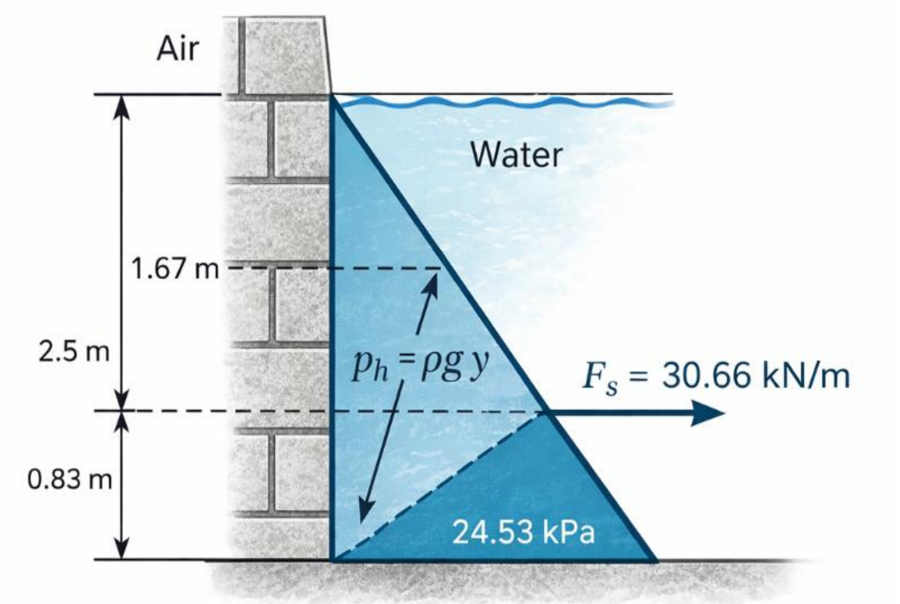

Figure 6. Idealized hydrostatic pressure distribution and resultant hydrostatic force acting on the dam face.

Engineering Interpretation

From an engineering point of view, the analytical methods remain useful for rapid and practical estimation of dynamic pressure levels. Their main advantage lies in their simplicity and ease of implementation. However, the present comparison shows that these methods provide idealized pressure distributions and do not fully represent the strongly localized character captured by the CFD model. In particular, the Fluent result at $t = 15.3$ shows a narrow and pronounced local peak, whereas the analytical curves remain smoother and more distributed along the plotted depth coordinate. This suggests that the analytical approaches are more appropriate for preliminary or conservative estimation of the dynamic component, while CFD-based analysis is more suitable for identifying local and time-dependent pressure concentrations on the dam face. Another important outcome is that the hydrostatic load is not negligible when compared with the earthquake-induced dynamic increment. As shown in Table 3, the base hydrostatic pressure for the adopted water depth is 24.53 kPa, whereas the main CFD-based dynamic peak is approximately 12.0 kPa. Therefore, the pressure demand on the dam face should not be interpreted only through the dynamic increment; instead, hydrostatic and hydrodynamic effects should be considered together. Accordingly, the Westergaard, Von Kármán, and Zangar methods may be considered suitable for preliminary and practical estimation of the dynamic component, whereas CFD-based modeling provides a more realistic basis for evaluating transient pressure localization and time-dependent wall-pressure evolution.

Conclusion

The main conclusions of this study can be summarized as follows:

1. The ANSYS Fluent analyses showed that the dynamic pressure distribution on the dam face is strongly time-dependent under earthquake excitation, and the most critical responses were observed at $t = 15.3$ sand $t = 15.6$ s.
2. The primary CFD-based dynamic peak was approximately **11.9–12.0 kPa** at $t = 15.3$ s, while the secondary critical response at $t = 15.6$ was approximately **4.2–4.3 kPa**.
3. Among the three analytical methods considered in the study, the **Von Kármán** and **Zangar** approaches showed closer agreement with the primary Fluent peak than the **Westergaard** approach in terms of peak dynamic-pressure magnitude.
4. The analytical methods provide smooth and idealized pressure distributions, whereas the CFD model reveals localized and transient pressure concentrations that vary during the excitation. Therefore, analytical

formulations are useful for preliminary assessment, but they do not fully represent the time-dependent character of the hydrodynamic response.

5. For the adopted water depth of **2.5 m**, the hydrostatic base pressure was calculated as **24.53 kPa**, and the resultant hydrostatic force per unit width was **30.66 kN/m**. This indicates that the hydrodynamic effect acts as a significant transient increment superimposed on an already substantial hydrostatic load.
6. The results confirm that a realistic seismic assessment of the dam face should consider the combined action of hydrostatic and hydrodynamic pressures rather than evaluating the dynamic component alone.

Recommendations

Future studies should focus on obtaining direct CFD-based force and pressure-center data from exported numerical results. In addition, dam flexibility, different reservoir levels, and multiple earthquake records should be considered in order to improve the physical realism of the analysis. The applicability of the analytical methods may also be further examined for inclined dam faces and different geometric configurations. Finally, hydrostatic and hydrodynamic effects should be assessed together for a more realistic evaluation of the total pressure demand acting on dam surfaces.

Scientific Ethics Declaration

* The authors declare that the scientific ethical and legal responsibility of this article published in EPSTEM journal belongs to the authors.

Conflict of Interest

* The authors declare that they have no conflicts of interest.

Funding

* No specific financial support was received for this study from any public, commercial, or not-for-profit funding organization.

Acknowledgements or Notes

* This article was presented as an oral presentation at the International Conference on Basic Sciences and Technology (www.icbast.net) held in Konya/Türkiye on April 02-05, 2026.

References

Ansys, Inc. (2025). *Ansys fluent user's guide* (Release 2025 R2). Canonsburg, PA: Ansys, Inc.

Chopra, A. K. (1967). Hydrodynamic pressures on dams during earthquakes. *Journal of the Engineering Mechanics Division, ASCE, 93*(EM6), 205–223.

Goldaran, R. (2022). Fluid–structure interaction: Impact of reservoir simulation approach considering far-field boundary condition in dam seismic response. *The Eurasia Proceedings of Science, Technology, Engineering & Mathematics, 21*, 88–95.

Housner, G. W. (1957). Dynamic pressures on accelerated fluid containers. *Bulletin of the Seismological Society of America, 47*(1), 15–35.

Jawad, A. A., Hassan, W. H., & Fattah, M. Y. (2021). Numerical analysis of a zoned earth dam considering hydrodynamic force during the earthquake excitation. *Journal of Physics: Conference Series, 1973*, 012183.

Von Kármán, T. (1933). The hydrodynamic pressure on dams during earthquakes. *Bulletin of the Seismological Society of America, 23*(3), 122–126.

Westergaard, H. M. (1933). Water pressures on dams during earthquakes. *Transactions of the American Society of Civil Engineers, 98*, 418–433.

Ye, J., Zhou, H., & Zhou, X. (2023). Hydrodynamic pressure on lateral side of dam excited by harmonic seismic vibration: A novel formulation. *Soil Dynamics and Earthquake Engineering, 164*, 107626.

Author(s) Information

Ali Yıldız
Konya Technical University, Faculty of Engineering and Natural Sciences, Department of Civil Engineering
Konya, Türkiye
ORCID iD: https://orcid.org/0000-0002-6909-6114
*Contact e-mail: *ayildiz@ktun.edu.tr*

Mustafa Kocer
Konya Technical University, Faculty of Engineering and Natural Sciences, Department of Civil Engineering
Konya, Türkiye
ORCID iD: https://orcid.org/0000-0002-5505-2065

Gulnaz Donmez
Konya Technical University, Faculty of Engineering and Natural Sciences, Department of Civil Engineering
Konya, Türkiye
ORCID iD: https://orcid.org/0009-0001-8191-3623

*Corresponding author(s) contact email

To cite this article:

Yildiz, A., Donmez, G., & Kocer, M. (2026). Comparative analysis of earthquake-induced hydrodynamic pressures in dam–reservoir systems using CFD and analytical methods. *The Eurasia Proceedings of Science, Technology, Engineering and Mathematics (EPSTEM), 40*, 129–139.